Research Square

Preprints are preliminary reports that have not undergone peer review.
They should not be considered conclusive, used to inform clinical practice,
or referenced by the media as validated information.

# Patho-morphogenetic remodeling of a severely atrophic unilateral right lower limb: a calibrated gross–radiographic case report

**Zezhou Xu**
Changsha Medical University
**Xiaoxuan Xiong**
Changsha Medical University
**Xianzhi Zhou**
Changsha Medical University
**Yifan Wang**
Changsha Medical University
**Haodong Chen**
Changsha Medical University
**Bing Li**
513809252@qq.com
Changsha Medical University

**Case Report**

**Keywords:** Cadaver, Lower extremity, Muscle atrophy, Osteopenia, Plantar flexion

**Posted Date:** November 6th, 2026

**DOI:** https://doi.org/10.21203/rs.3.rs-11307337/v1

**License:** This work is licensed under a Creative Commons Attribution 4.0 International License.
Read Full License

**Additional Declarations:** No competing interests reported.

# Abstract

Bone and muscle remodel jointly in response to neural drive and mechanical loading, and both undergo profound degeneration under chronic disuse or denervation. Quantitatively calibrated descriptions of such extreme remodeling at single-limb level, integrating radiology with gross and cross-sectional anatomy, remain scarce. We report a formalin-fixed right lower limb from an elderly male cadaver showing severe unilateral atrophy. Premortem anteroposterior radiographs of the knee and foot, each bearing a 10-mm scale marker, were used to derive a distal-diaphyseal cortical index for the tibia and fibula, the ankle plantar-flexion angle, and heel-pad thickness. The limb then underwent layered dissection and mid-thigh cross-sectioning to quantify compartmental muscle area fractions. The distal tibial and fibular cortical indices were 0.131 and 0.433, respectively, indicating extreme cortical thinning of the tibia with relatively spared fibular cortex. The ankle was fixed in approximately 34.9° of plantar flexion, and the heel pad measured 9.8 mm. Only about 12.5% of the mid-thigh cross-section consisted of contractile muscle (anterior compartment 13.3%, medial 3.3%, posterior 20.4%), with extensive fatty replacement. Radiographs and anatomical findings were concordant for diffuse osteopenia, tendon prominence, and severe myosteatosis. Taken together, the calibrated metrics support long-standing disuse with probable partial denervation of this limb. Beyond documenting an extreme phenotype of coupled bone–muscle degeneration, this case illustrates a simple, reproducible workflow for quantitative analysis in single-case musculoskeletal pathology using visible scale references and explicitly defined regions of interest.


# Introduction

Bone and skeletal muscle form a mechanically and metabolically coupled organ system. When habitual strains fall below mechanostat thresholds, trabecular rarefaction and cortical thinning follow; restoration of loading can partially reverse these changes (Frost 2003; Robling and Turner 2009). Chronic disuse or denervation accelerates muscle proteolysis, fibrosis, and fatty infiltration with loss of contractile tissue (Dulor et al. 1998; Carlson 2014), and this remodeling is further shaped by muscle–bone crosstalk through myokines and osteokines (Rolvien et al. 2020; Rolvien and Amling 2022). Clinical imaging studies in stroke and spinal cord injury have highlighted that osteopenia and intramuscular fat accumulation commonly coexist in chronically unused limbs (Ryan et al. 2002; Gorgey and Dudley 2007).

Despite this, integrative analyses that are quantitatively calibrated across radiographic, gross, and sectional anatomical levels remain uncommon in the anatomical literature. Most reports emphasize either imaging or dissection, whereas single-case musculoskeletal pathology can benefit from an explicit, measurement-based workflow.

Here, we describe a cadaveric right lower limb with severe unilateral atrophy and diffuse osteopenia. By combining premortem radiographs calibrated with embedded scale markers and postmortem gross and cross-sectional anatomy, we derive cortical indices, joint posture, heel-pad thickness, and compartmental muscle area fractions. This case represents an extreme example of disuse-related

patho-morphogenetic remodeling and serves as a template for quantitative anatomical analysis in individual specimens.

## Case report

# Donor and ethical context

The lower-limb specimen used in this study was obtained from the voluntary body donation program of Changsha Medical University. During life, the donor had provided written informed consent for body donation and for the use of the body in medical education and research. All potentially identifiable personal information was removed before the present study was conducted. Cadaveric dissection and sampling were carried out in the Department of Human Anatomy according to the routine rules for medical student dissection and the institutional regulations on the research use of human remains. According to the Institutional Review Board of Changsha Medical University, anonymized studies based exclusively on donated cadaveric material do not require additional project-specific ethical approval. Nonetheless, the authors confirm that every effort was made to comply with all applicable local regulations and international ethical guidelines concerning the use of human cadaveric donors in anatomical research.

## Radiographic assessment and calibrated measurements

Digital copies of the knee and foot/ankle radiographs were imported into ImageJ2 (Fiji distribution) for analysis. Spatial calibration was performed using the embedded 10-mm scale on each image (6.20 pixels/mm for the foot image and 23.10 pixels/mm for the knee image). A distal-diaphyseal cortical index (CI) was measured for both tibia and fibula on the foot radiograph. CI was defined as (D_outer − D_medullary)/D_outer, where D_outer is the outer bone diameter and D_medullary the medullary canal diameter at a standardized level just proximal to the ankle joint, measured along a line perpendicular to the long axis. The ankle plantar-flexion angle was constructed between the longitudinal axis of the tibia and that of the second metatarsal. Heel-pad thickness was measured as the maximal perpendicular distance from the inferior calcaneal cortex to the external skin margin of the heel.

**Knee radiograph (**Fig. 1A**).** The distal femur and proximal tibia showed marked osteopenia with diffuse trabecular rarefaction (A1) and demineralized subchondral bone (A2), yet preserved joint alignment (A3) and no evidence of fracture (A4) or periosteal reaction (A5).

**Foot/ankle radiograph (**Fig. 1B**).** The tarsal bones, metatarsals, and phalanges exhibited globally reduced bone density with thin cortical rims; the calcaneus was particularly osteopenic (B3). Calibrated measurements on this image yielded a distal tibial CI of 0.131 indicating extreme cortical thinning (B1) and a distal fibular CI of 0.433 indicating moderate thinning (B2). The heel-pad thickness was 9.8 mm (B4), and the ankle was fixed in an equinus posture of ~ 34.9° plantar flexion relative to the tibial axis (B5).

## Gross morphology of the lower limb

Externally, the right lower limb had a “skin-and-bone” appearance with striking loss of muscle bulk (Fig. 1C). In the thigh, the quadriceps were markedly shrunken, producing loosely draped skin and a prominent patella (C1). Posteriorly, hamstring tendons were clearly visible beneath the skin (C2). In the calf, the gastrocnemius and soleus were extremely slender, and the normal convex bulge of the calf was flattened (C3). The Achilles tendon appeared narrow and sharply delineated (C4). The ankle and foot were maintained in equinus, with the toes slightly flexed (C5). On the dorsum of the foot, extensor tendons were clearly visible under thinned soft-tissue envelopes. No scars or overt traumatic lesions were observed on the skin to suggest prior surgery or major injury.

## Cross-sectional anatomy and muscle area fractions

A transverse section was made at approximately 50% of femoral length, midway between the inguinal region and the superior pole of the patella, to obtain a mid-thigh cross-section. The section was photographed with an embedded scale bar, and anterior, medial, and posterior compartments were delineated according to fascial boundaries. Within each compartment, residual red-brown muscle tissue was separated from pale yellow-white adipose and fibrous tissue by a combination of visual inspection and digital thresholding. Compartmental muscle area fractions were computed as (muscle area / total compartment area) × 100%. Measurement precision and first-order uncertainties due to pixel calibration and landmark placement were documented, with cortical indices recorded to three decimal places, angles and percentages to one decimal place, and linear dimensions to 0.1 mm.

The mid-thigh section confirmed global muscle wasting with extensive fatty replacement (Fig. 1D). In the anterior compartment (quadriceps), only small islands of residual muscle remained within a predominantly adipose background (D1). The medial compartment (adductors) was near-completely replaced by fat (D2). The posterior compartment (hamstrings), although relatively better preserved, still showed substantial atrophy with interspersed fat streaks (D3). Quantitatively, contractile muscle area fractions were 13.3% in the anterior compartment, 3.3% in the medial compartment, and 20.4% in the posterior compartment. Considering the entire cross-section, ~ 12.5% of the area consisted of contractile muscle (D4), the remainder being adipose/fibrous replacement tissue (D5).

Table 1 summarizes the calibrated indices and their qualitative interpretation, including distal tibial and fibular cortical indices, heel-pad thickness, ankle plantar-flexion angle, and compartmental muscle area fractions, together with estimated measurement uncertainties.

Table 1
Calibrated quantitative indices

| Metric | Measured value | Interpretation |
|---|---|---|
| Distal tibia cortical index (CI) | 0.131 | Extremely thin cortex (severe osteopenia in distal tibia) |
| Distal fibula cortical index (CI) | 0.433 | Moderately thinned cortex (fibula relatively less affected) |
| Heel-pad thickness | 9.8 mm | Reduced heel fat pad (consistent with chronic disuse; AP view measurement) |
| Ankle plantar-flexion angle | ~ 34.9° | Fixed equinus deformity (permanent plantar flexion of ankle) |
| Contractile muscle area fraction – Anterior thigh | 13.3% | Severe anterior compartment atrophy (almost 87% replaced by fat/connective tissue) |
| Contractile muscle area fraction – Medial thigh | 3.3% | Near-complete medial compartment atrophy |
| Contractile muscle area fraction – Posterior thigh | 20.4% | Posterior compartment atrophy (better preserved than anterior/medial) |
| Contractile muscle area fraction – Whole slice | ~ 12.5% | Global muscle loss (only one-eighth of thigh cross-section is contractile muscle) |
| Calibration and uncertainty: Radiographic pixel calibration ± 1 pixel ( ≈ ± 0.005 in CI). Heel-pad thickness may be underestimated in AP view (± 0.2 mm). Ankle angle measurement uncertainty ± 0.5–1.0°. Planimetry variability present but does not affect overall patterns. | | |

## Discussion

# Integrated interpretation of bone and muscle remodeling

This case demonstrates an extreme phenotype of coupled bone and muscle degeneration in a single lower limb. The very low distal tibial cortical index (0.131) reflects severe disuse osteoporosis at the distal skeleton, consistent with long-term unloading and reduced mechanostat signaling (Frost 2003; Robling and Turner 2009). The mid-thigh cross-section, with only ~ 12.5% of the area composed of contractile muscle and the remainder replaced by adipose/fibrous tissue, is typical of chronic denervation or disuse atrophy (Dulor et al. 1998; Carlson 2014) and parallels clinical observations in immobilization, stroke, or spinal cord injury, where heightened intramuscular fat accompanies profound muscle loss (Ryan et al. 2002; Gorgey and Dudley 2007).

Interestingly, the posterior thigh compartment retained a slightly higher muscle fraction than the anterior and medial compartments, suggesting partial preservation of some muscle groups (e.g., hamstrings) or differential neural involvement. The fixed equinus deformity (~ 35° plantar flexion) points to adaptive shortening of the triceps surae–Achilles complex and relative weakness or paralysis of dorsiflexors, a

common pattern in long-standing paralysis or immobilization. Overall, the concordant osteopenia, myosteatosis, tendon prominence, and joint posturing depict a limb that has been functionally unused for a prolonged period, with bone and muscle undergoing parallel degeneration in line with contemporary models of musculoskeletal crosstalk (Rolvien et al. 2020; Rolvien and Amling 2022).

## Etiological considerations

The precise cause of this unilateral atrophy cannot be determined because no clinical records accompanied the donor. Several etiological scenarios, however, are consistent with the anatomical and radiographic findings. A chronic peripheral neuropathy or plexopathy involving lumbosacral nerves could produce profound denervation atrophy, with compartment-specific severity depending on the nerves involved. No gross neuroma or obvious nerve disruption was detected on dissection, but an old sciatic lesion or a remote anterior horn cell disease (e.g., poliomyelitis confined predominantly to one side) could lead to the near-complete muscle loss seen here.

Prolonged immobilization or casting, for example following joint injury or stroke-related hemiparesis, is another plausible contributor. Extended non-weight-bearing would explain the diffuse osteopenia, while lack of active use would drive muscle wasting and tendon shortening. Complex regional pain syndrome might also be considered, given its association with regional osteopenia and soft-tissue change; however, typical features such as severe pain and autonomic skin alterations cannot be assessed in a cadaver, and CRPS alone rarely produces such extreme muscle loss without sustained disuse. Primary myopathies usually present bilaterally and do not cause focal osteoporosis; therefore, an isolated myopathic process is unlikely to be the dominant mechanism. Taken together, a combination of chronic disuse (unloading) and neurological impairment—whether upper motor neuron, lower motor neuron, or both—appears to be the most consistent explanation for the observed remodeling.

## Methodological and educational aspects

From a methodological perspective, we opted to derive cortical indices from distal tibial and fibular profiles on the available foot radiograph rather than mid-shaft regions. While mid-shaft indices are more standard for diaphyseal bone evaluation, the distal approach provided unobstructed profiles at a location where calibration markers were clearly visible and yielded values that qualitatively mirrored the generalized osteopenia. Similarly, the AP radiograph is not ideal for heel-pad thickness or ankle angle assessment—weight-bearing lateral views would be preferable—but in this context, AP-based measures still offer useful approximations, especially when their uncertainties are explicitly reported.

For the soft-tissue analysis, single-observer planimetry and semi-subjective thresholding inevitably introduce variability. However, the contrast between residual muscle and fat in this limb was so marked that broad patterns are robust to modest measurement noise. Future cadaveric studies or clinical case reports could supplement such measurements with dual-energy X-ray absorptiometry for bone density or

MRI for muscle volume and composition, providing more precise quantitation while retaining the practical advantages of simple radiographs and photographs.

Beyond its research value, this case has clear educational implications. The combination of calibrated radiographs, gross photographs, and cross-sections with visible scale bars and clearly defined regions of interest offers students a concrete, quantitative view of disuse-related remodeling. It bridges classroom discussions of mechanostat theory and muscle–bone crosstalk with tangible anatomy in a single limb.

# Limitations

As with any single-case cadaveric report, generalizability is limited. The lack of clinical history prevents definitive etiological diagnosis and correlation with functional deficits. Cortical indices were derived from a distal site rather than standard mid-shaft positions and should be interpreted as relative indicators of cortical thinning. Heel-pad thickness and ankle angle were measured on non-weight-bearing AP radiographs and thus are approximations rather than gold-standard values. Achilles tendon length and cross-sectional area were not quantified, so tendon remodeling is documented qualitatively. Finally, muscle–fat segmentation was performed by a single observer and remains partially subjective despite the stark tissue contrast. Nevertheless, the internal consistency of radiographic and anatomical findings supports the overall interpretation of profound chronic disuse and partial denervation.

## Conclusion

This case report documents an extreme example of unilateral lower-limb disuse atrophy and osteopenia, integrating calibrated radiography with detailed gross and cross-sectional anatomy. Distal tibial and fibular cortical indices, thin heel pad, fixed equinus posture, and dramatically reduced thigh muscle area fractions collectively indicate long-standing unloading with probable partial denervation. In addition to illustrating the coupled degeneration of bone and muscle under chronic disuse, the study demonstrates a straightforward quantitative workflow based on visible scale markers, explicit regions of interest, and reported uncertainties. Such an approach can enhance the anatomical and clinical value of single-specimen musculoskeletal case reports and foster more data-driven teaching of pathologic anatomy.

## Abbreviations

AP, anteroposterior; CI, cortical index.

## Declarations

**Ethics approval and consent to participate**

The lower-limb specimen used in this study was obtained from the voluntary body donation program of Changsha Medical University. During life, the donor had provided written informed consent for body donation and for the use of the body in medical education and research. All potentially identifiable

personal information was removed before the present study was conducted. Cadaveric dissection and sampling were carried out in the Department of Human Anatomy according to the routine rules for medical student dissection and the institutional regulations on the research use of human remains. According to the Institutional Review Board of Changsha Medical University, anonymized studies based exclusively on donated cadaveric material do not require additional project-specific ethical approval.

**Consent for publication**

Written informed consent was obtained from the patient for publication of this case report and any accompanying images.

# Competing Interests

The authors declare that they have no competing interests.

# Clinical Trial Number

Not applicable.

# Funding

The authors received no financial support for the research, authorship, and/or publication of this article.

# Author Contribution

Ze-Zhou Xu conceived and supervised the study. Ze-Zhou Xu and Bing Li performed the dissection and imaging. Xiao-Xuan Xiong and Yi-Fan Wang contributed to data analysis, literature review, and interpretation. Hao-Dong Chen and Xian-Zhi Zhou assisted with image calibration and planimetry. All authors participated in drafting and revising the manuscript and approved the final version.

# Acknowledgement

We sincerely thank those who donated their bodies to science so that anatomical research could be performed. Results from such research can increase overall knowledge and ultimately improve patient care; these donors and their families therefore deserve our highest gratitude. We also thank the staff and colleagues of the anatomy laboratory at Changsha Medical University for assistance with specimen preservation and dissection.The authors express their deepest gratitude to the individuals who donated their bodies and to their families. Their generous contribution makes it possible to perform detailed

anatomical research, which can expand our understanding of human morphology and ultimately improve the safety and quality of patient care.

# Data Availability

All relevant data generated or analyzed during this study (including calibrated images, regions of interest, and quantitative datasets) are available from the corresponding author on reasonable request.

## References


1. Agur AMR, Dalley AF. Grant's Atlas of Anatomy. 14th ed. Philadelphia: Wolters Kluwer; 2017.
2. Carlson BM. The biology of long-term denervated skeletal muscle. Eur J Transl Myol. 2014;24:85–92. 10.4081/ejtm.2014.3293.
3. Dulor JP, Cambon B, Vigneron P, Reyne Y, Nougues J, Casteilla L, Bacou F. Expression of specific white adipose tissue genes in denervation-induced skeletal muscle fatty degeneration. FEBS Lett. 1998;439:89–92. 10.1016/S0014-5793(98)01216-2.
4. Frost HM. Bone's mechanostat: a 2003 update. Anat Rec A. 2003;275:1081–101. 10.1002/ar.a.10119.
5. Gorgey AS, Dudley GA. Skeletal muscle atrophy and increased intramuscular fat after incomplete spinal cord injury. Spinal Cord. 2007;45:304–9. 10.1038/sj.sc.3102038.
6. Robling AG, Turner CH. Mechanical signaling for bone modeling and remodeling. Crit Rev Eukaryot Gene Expr. 2009;19:319–38. 10.1615/CritRevEukarGeneExpr.v19.i4.50.
7. Rolvien T, Milovanovic P, Busse B, Amling M, et al. Musculoskeletal crosstalk and the pathogenesis of disuse. Curr Osteoporos Rep. 2020;18:541–51. 10.1007/s11914-020-00600-3.
8. Rolvien T, Amling M. Disuse osteoporosis: clinical and mechanistic insights. Calcif Tissue Int. 2022;110:592–604. 10.1007/s00223-021-00913-2.
9. Ryan AS, Dobrovolny CL, Smith GV, Silver KH, Macko RF. Hemiparetic muscle atrophy and increased intramuscular fat in stroke patients. Arch Phys Med Rehabil. 2002;83:1703–7. 10.1053/apmr.2002.36399.


## Figures

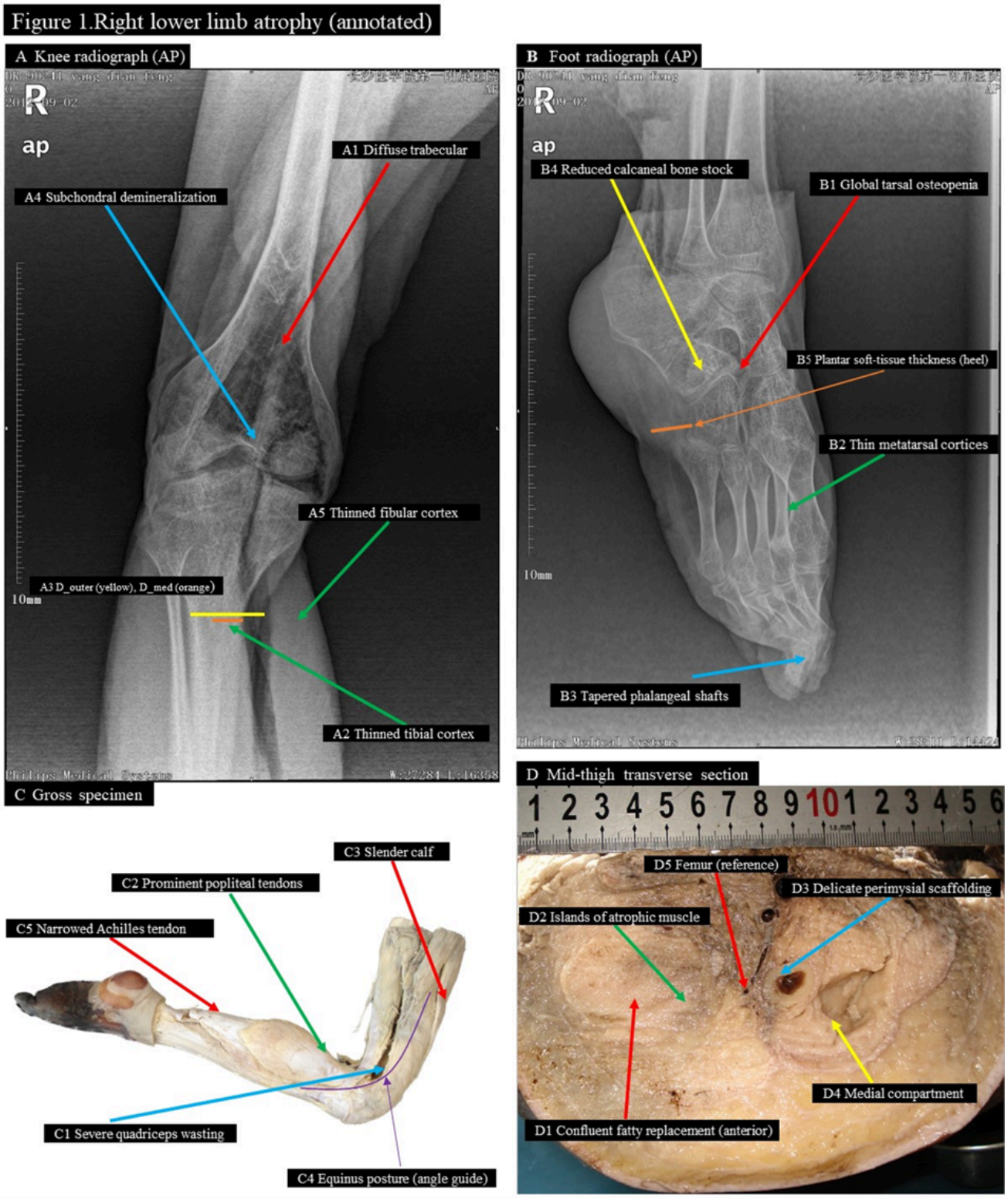



**Figure 1**

**Right lower limb atrophy (integrated radiographic, gross, and cross-sectional views).**
**(A) Anteroposterior radiograph of the right knee.**A1: diffuse trabecular rarefaction; A2: demineralized subchondral bone; A3: preserved joint alignment; A4: no fracture; A5: no periosteal reaction.
**(B) Anteroposterior radiograph of the right foot and ankle.** B1: extremely thinned distal tibial cortex (cortical index 0.131); B2: moderately thinned distal fibular cortex (cortical index 0.433); B3: pronounced

calcaneal osteopenia; B4: thin heel pad (9.8 mm); B5: fixed equinus deformity (~34.9° plantar flexion). **(C) Gross morphology.** C1: prominent patella from severe quadriceps wasting; C2: visible hamstring tendons; C3: flattened calf due to gastrocnemius–soleus atrophy; C4: narrow Achilles tendon; C5: equinus foot posture with toe flexion. **(D) Mid-thigh transverse section.** D1: anterior compartment—small residual muscle islands amid adipose; D2: medial compartment—near-complete fatty replacement; D3: posterior compartment—partial muscle preservation; D4: residual contractile muscle ~12.5% of total area; D5: fatty/fibrous replacement ~87.5%. (Scale bars: 10 mm in radiographs; 1 cm in gross and sectional images.)